European Review for Medical and Pharmacological Sciences 2023; 27: 1954-1970

ELOVL fatty acid elongase 7 (*ELOVL7*), upregulated by *Mdr2*-knockout, predicts advanced liver fibrosis in patients with chronic hepatitis B

W.-M. WANG[1], Z.-G. YANG[2], C. LIU[3], Q. DONG[1]

[1]Department of Traditional Chinese Medicine, Beijing Tian Tan Hospital, Capital Medical University, Beijing, China
[2]Department of Integrative Medicine, Shanghai Public Health Clinical Center, Fudan University, Shanghai, China
[3]Department of Infectious Disease, Putuo Hospital, Shanghai University of Traditional Chinese Medicine, Shanghai, China

Abstract. – OBJECTIVE: This study aims to investigate the correlations between gene alterations induced in *Mdr2*-knockout (Mdr$^{2-/-}$) models and liver fibrosis.

SUBJECTS AND METHODS: The overlapping genes in *Mdr2*$^{-/-}$ models were determined and included in logistic regression analysis to identify potential candidates for predicting liver fibrosis. Correlations between the expression levels of the identified candidates and hepatic stellate cells (HSCs) were addressed. Functional enrichment of the identified candidates was also evaluated *via* bioinformatic analysis.

RESULTS: Twenty-two overlapping genes in the GSE4612, GSE8642 and GSE14539 datasets were identified. Univariate and multivariate analysis indicated that ELOVL fatty acid elongase 7 (*ELOVL7*) was significantly associated with liver fibrosis S ≥ 2 (OR = 11.8, 95% CI = 2.0 - 69.2, $p = 0.006$). *ELOVL7* was significantly upregulated in patients with various types of liver injury including hepatitis B virus (HBV) infection and fatty liver diseases, and in multiple liver injury models, including bile duct ligation (BDL), carbon tetrachloride (CCl4) and paracetamol injection-induced liver damage models (all $p < 0.05$). The *ELOVL7* levels were significantly higher in HSCs than in other liver cells (all $p < 0.05$) and were significantly upregulated in activated HSCs compared to quiescent HSCs (all $p < 0.05$). In addition, *ELOVL7* expression was positively associated with transforming growth factor β (TGFβ) and bone morphogenic protein 9 (BMP9) expression and negatively associated with BMP7 expression. Bioinformatic analysis of functional enrichment indicated that *ELOVL7* is mainly involved in fatty acid synthesis and metabolism.

CONCLUSIONS: *ELOVL7* could accurately predict advanced liver fibrosis. It might be involved in the activation of HSCs and the TGFβ signaling pathway.

Key Words:
ELOVL7, Mdr2, Liver fibrosis, Cirrhosis, Hepatic stellate cells, TGFβ, Fatty acid synthesis, Metabolism.

Introduction

Fibrosis and the resulting organ injury and failure are responsible for at least one third of all deaths worldwide[1,2], and its incidence is increasing[3]. Liver fibrosis occurs in response to various etiologies of chronic liver damage, including viral hepatitis, fatty liver diseases, alcoholic hepatitis, autoimmune and metabolic liver diseases, and toxic liver injury[4]. The liver disease progresses through various stages, among which liver fibrosis is the pivotal step[5]. Fibrosis is stimulated by chronic inflammation, which causes quiescent hepatic stellate cells (HSCs) to be activated, induces the expression of profibrotic factors and promotes liver damage progression[6], resulting in the destruction of liver structures, the replacement of liver parenchyma by fibrous tissue, the development of regenerative nodules and hepatic dysfunction[7].

Robust experimental models of fibrosis are emerging and provide promising approaches for understanding the mechanisms underlying liver fibrosis and the application of potential antifibrotic strategies[1]. As classical models of cholestatic liver disease, multidrug resistance protein 2 knockout (*Mdr2*$^{-/-}$) mouse models are widely used for research[8,9] on various liver diseases including liver fibrosis. Compared to normal livers, the livers of *Mdr2*$^{-/-}$ mice frequently exhibit infiltration of hepatic neutrophils, accumulation of proinflammatory cytokines, and

Corresponding Author: Qian Dong, MD, Ph.D; e-mail: dongqian1982@sina.com

increased numbers of monocyte-derived macrophages[9-12]. In addition, the activation of fibroblasts around the ducts, and periductal fibrosis have been confirmed[13] in 8-week-old *Mdr2*$^{-/-}$ mice. According to the pathogenic features of *Mdr2*$^{-/-}$ mice, gene alterations in this model are expected to be closely associated with liver fibrosis progression.

It is recognized that liver fibrosis is a precursor to cirrhosis. Early diagnosis and assessment of liver fibrosis is critical for reversal of liver fibrosis and cirrhosis[4,14]. In the present study, we aimed to elucidate the gene alterations induced in *Mdr2*$^{-/-}$ mice and investigate the correlations between these alterations and liver fibrosis progression, in the hope that the findings may provide novel diagnostic candidates and therapeutic targets as well as useful insights into the pathogenesis and mechanisms of liver fibrosis.

Table I. Clinical characteristics of 124 HBV-related liver fibrosis patients.

Variables	n = 124
Age, median (Interquartile range, IQR)	40 (23.51)
Male, n (%)	87 (70.2)
S stage, n (%)	
0	42 (33.9)
1	20 (16.1)
2	34 (27.4)
3	18 (14.5)
4	10 (8.1)
G grade, n (%)	
0	37 (29.8)
1	33 (26.6)
2	34 (27.4)
3	15 (12.1)
4	5 (4.0)

Subjects and Methods

Ethics Statement

Written informed consent was obtained from all participants[15]. The protocol of this secondary analysis was reviewed and approved by the Ethics Committee of Beijing Tian Tan Hospital, Capital Medical University.

Mdr2$^{-/-}$ Mouse Sequencing Datasets

As of April 21, 2022, 30 series were identified with the keywords "*Mdr2*" in the Gene Expression Omnibus (GEO, available at: https://www.ncbi.nlm.nih.gov/geo/) database[16,17]. Seventeen series with expression profiling by array were screened further. The source organism of all 17 series was *Mus musculus*. Only series containing raw.CEL files and platforms with "ID", "Gene symbol", and "ENTREZ_GENE_ID" terms were included in this analysis. Finally, GSE4612[18], GSE8642[19] and GSE14539[20] were included in the analysis. The details of the GEO series included in this analysis are summarized in **Supplementary Table I**.

Patients and Outcome Definition

The GSE84044[15] dataset was used to screen candidate molecules for predicting liver fibrosis[15]. As we previously reported[21], liver biopsy samples from 124 patients with chronic hepatitis B (CHB) were included in this dataset. The clinical characteristics, including the age, gender and histopathological diagnosis results, of these CHB patients were available[21]. The diagnosis of CHB was made according to the criteria of the Asian Pacific Association for the Study of the Liver (APASL)[22]. Patients with the following characteristics were excluded from the study: 1) use of any antiviral therapies or immunosuppressive drugs within six months before sampling and 2) lack of hepatitis B virus (HBV) infection, human immunodeficiency virus (HIV) infection, autoimmune liver disease, drug-induced liver injury, alcoholic liver disease or hepatocellular carcinoma. The histopathological diagnosis of all liver biopsies was confirmed by two experienced pathologists from the Pathology Department of Shanghai Fudan University, School of Medicine. The fibrosis staging (Scheuer S) and inflammation grading (Scheuer G) were calculated according to the Scheuer scoring system, namely, S 0-4 and G 0-4[23,24]. The primary outcome was advanced liver fibrosis, which was defined as a histological fibrosis staging of $S \geq 2$. As stated by Wang et al[15], all subjects provided written informed consent. The study protocol was approved by the Ethics Committee of Ruijin Hospital, Shanghai Jiaotong University, School of Medicine.

Identification of Differentially Expressed Genes (DEGs)

This identification framework was used in all the GEO series included in this analysis. Raw.CEL files of the microarray data from each GEO dataset were subjected to quantile normalization with the robust multichip analysis (RMA) algorithm in the R package affy (available at: https://

www.r-project.org)[25]. Gene expression was compared with the Limma package (Bioconductor, Roswell Park Comprehensive Cancer Center, NY, USA)[26]. Missing gene expression data were imputed by the k-nearest neighbor method with the impute index in the R program[27]. All the platforms and samples of the GEO series were downloaded from https://www.ncbi.nlm.nih.gov/geo/. DEGs were identified as genes meeting the criteria of $|\log_2 FC| > 1.0$ and adjusted p-value < 0.05.

RNA Sequencing of Liver Fibrosis Samples

Eight liver biopsy samples from Putuo Hospital, Shanghai University of Traditional Chinese Medicine, namely, samples from 4 patients with liver fibrosis S ≥ 2 and 4 normal liver samples were sequenced. Whole-genome microarray expression profiling was conducted by Shanghai OE Biotech Co., Ltd (Shanghai, China) with the OE Biotech Human ceRNA Microarray Platform GPL28576. The raw microarray data have been deposited in the GEO database under accession series code GSE197112.

Enrichment of DEGs

The average $\log_2$-transformed fold changes in the expression of the overlapping DEGs were calculated in the GSE4612[18], GSE8642[19] and GSE14539 datasets[20]. The Gene Ontology (GO) Enrichment Analysis tool in the SRplot online server (available at: http://www.bioinformatics.com.cn/en) was used to identify the biological processes and molecular functions of these overlapping DEGs in mice.

Protein-Protein Interaction (PPI) of Candidates

The PPI of the identified candidates for predicting liver fibrosis was evaluated by STRING version 11.5 (available at: https://cn.string-db.org/)[28,29]. The sources used to identify active interactions in the PPI network included text mining, experiments, databases, co-expression, neighborhood, gene fusion, and co-occurrence analyses. The minimum required interaction score was 0.4. The Kyoto Encyclopedia of Genes and Genomes (KEGG) pathway, Reactome pathway and GO biological process enrichment of the genes in the PPI network were also determined with the STRING database.

Statistical Analysis

Differences in gene expression levels between the individual groups were analyzed using Student's *t*-test, the Mann-Whitney U test or two-way ANOVA, based on the variable type by GraphPad Prism 8 (GraphPad Software, La Jolla, CA, USA). Variables associated with the liver fibrosis stage were assessed by univariate and multivariate logistic regression analysis. The results are reported as odds ratios (ORs) with 95% confidence intervals (CIs). The OptimalCutpoints package[30] (available at: https://www.r-project.org) in the R program was used to perform ROC analysis to evaluate the predictive values of potential candidates for the liver fibrosis stage and inflammation grade, and the rmda package[31,32] (available at: https://www.r-project.org) was used for decision curve analysis (DCA) to reevaluate the predictive performance of the candidates. Correlation analysis was performed by the Spearman's method. Stata software version 16.1 (Stata Corp LLC, Texas, USA) was used for logistic regression and correlation analyses. A two-tailed $p < 0.05$ was considered significant.

Results

Overlapping DEGs in Mdr2 Knockout Mouse Models

The flow diagram of the study is summarized in Figure 1. In total, 2,481, 498 and 1,313 DEGs were identified in the GSE4612[18], GSE8642[19] and GSE14539[20] datasets, respectively. A Venn diagram was used to identify 22 overlapping DEGs among these three GEO series (Figure 2A). As detailed in Figure 1B, all 22 genes were significantly upregulated in the livers of 9-month-old *Mdr2*$^{-/-}$ mice compared to wild-type mice (all $p < 0.05$, GSE14539, Figure 2B). They were also significantly upregulated in 12-month-old compared to 3-month-old *Mdr2*$^{-/-}$ homozygous mice (all $p < 0.0001$, GSE4612, Figure 2B) and were significantly upregulated in tumor tissues compared to nontumor tissues in *Mdr2*$^{-/-}$ mice (all $p < 0.05$, GSE8642, Figure 2B). Enrichment analysis of the overlapping DEGs indicated that they were involved mainly in biological processes that included response to tumor necrosis factor, cellular response to tumor necrosis factor, and positive regulation of response to external stimulus, etc. (Figure 2C). The overlapping DEGs also had molecular functions that included structural constituent of cytoskeleton, cadherin binding, metalloendopeptidase activity, etc. (Figure 2D).

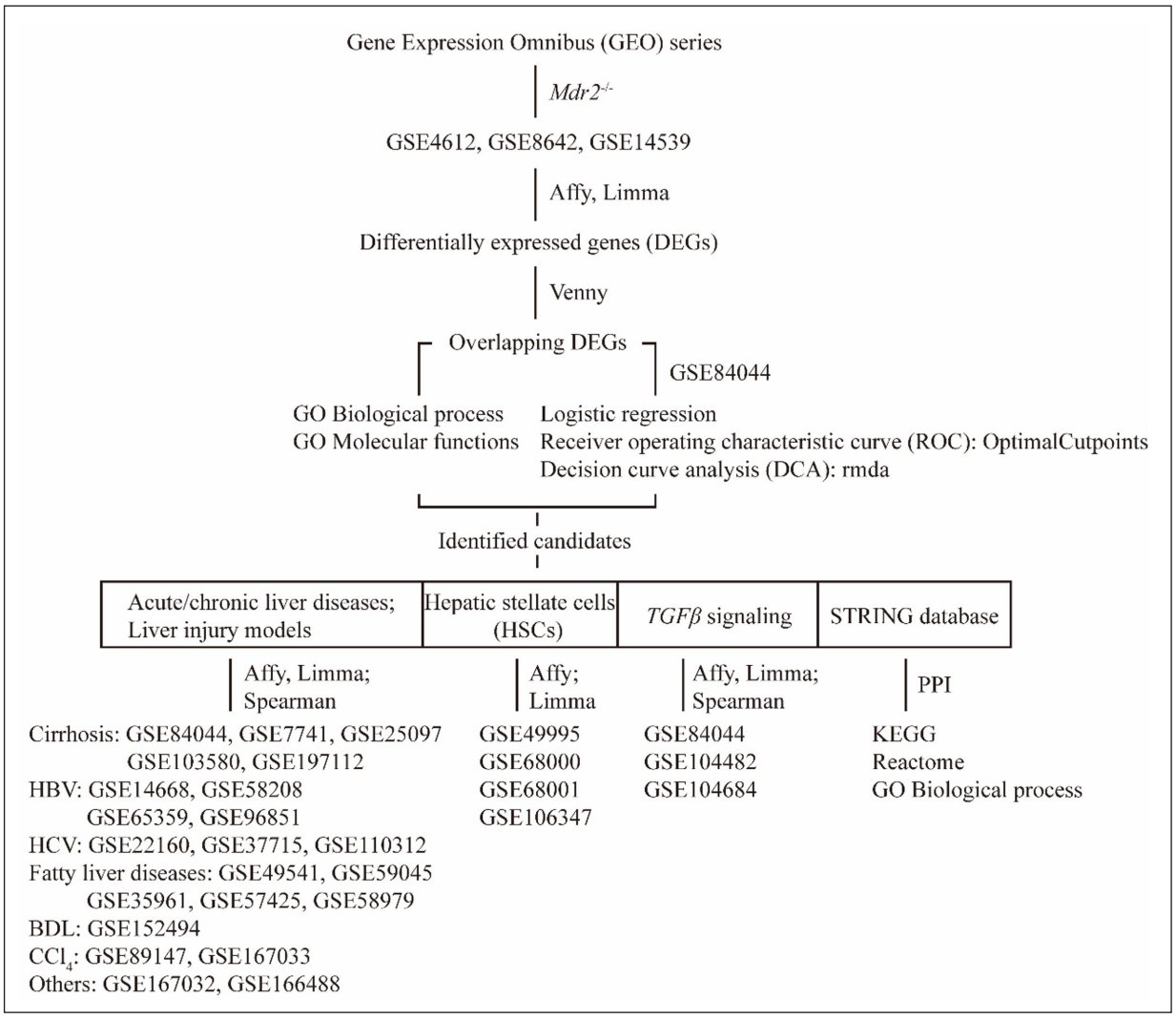

Figure 1. The flow diagram of the study.

Candidate Genes for Predicting Liver Fibrosis

In the liver fibrosis dataset GSE84044[15], the median age of the 124 CHB patients was 40 years, and 87 (70.2%) were male (Table I). The gene expression data of SDCBP2 were not available in the GSE84044 dataset. As summarized in Figure 3A, *TUBB6*, *RGS1*, *PROM1*, *CRIP2*, *COL4A5*, *TNFRSF12A*, *ELOVL7*, *ADAM10*, *FABP4*, *TMEM45B*, *CASP4*, and *LIMS1* were significantly overexpressed in the liver samples with S ≥ 2 (all $p < 0.05$, Figure 3A), and *PDK4*, *NTF3*, *NDRG1*, *AQP8* were significantly downregulated in liver samples with S < 2 (all $p < 0.05$, Figure 3A). Univariate logistic regression analysis revealed that age, *TUBB6*, *RGS1*, *PROM1*, *CRIP2*, *COL4A5*, *TNFRSF12A*, *ELOVL7*, *PDK4*, *NTF3*, *NDRG1*, *ADAM10*, *FABP4*, *TMEM45B*, *CASP4*, *AQP8*, and *LIMS1* were potential candidates for predicting liver fibrosis S ≥ 2 (all $p < 0.05$, Figure 3B). Multivariate logistic regression analysis indicated that *ELOVL7* upregulation was significantly associated with liver fibrosis S ≥ 2 (OR = 11.8, 95% CI = 2.0 - 69.2, $p = 0.006$, Figure 3C).

Predictive Performance of ELOVL7 for Liver Fibrosis and Liver Inflammation

To evaluate the predictive accuracy of *ELOVL7* for liver fibrosis and liver inflammation, we performed receiver operating characteristic (ROC) analysis and found that *ELOVL7* accurately predicted liver fibrosis S ≥ 2 [cutoff = 3.92, AUC = 0.9 (95% CI = 0.85 - 0.95), specificity = 0.87, sensitivity = 0.79, positive predictive value (PPV) = 0.81, and negative predictive value (NPV) = 0.86, Figure 4A].

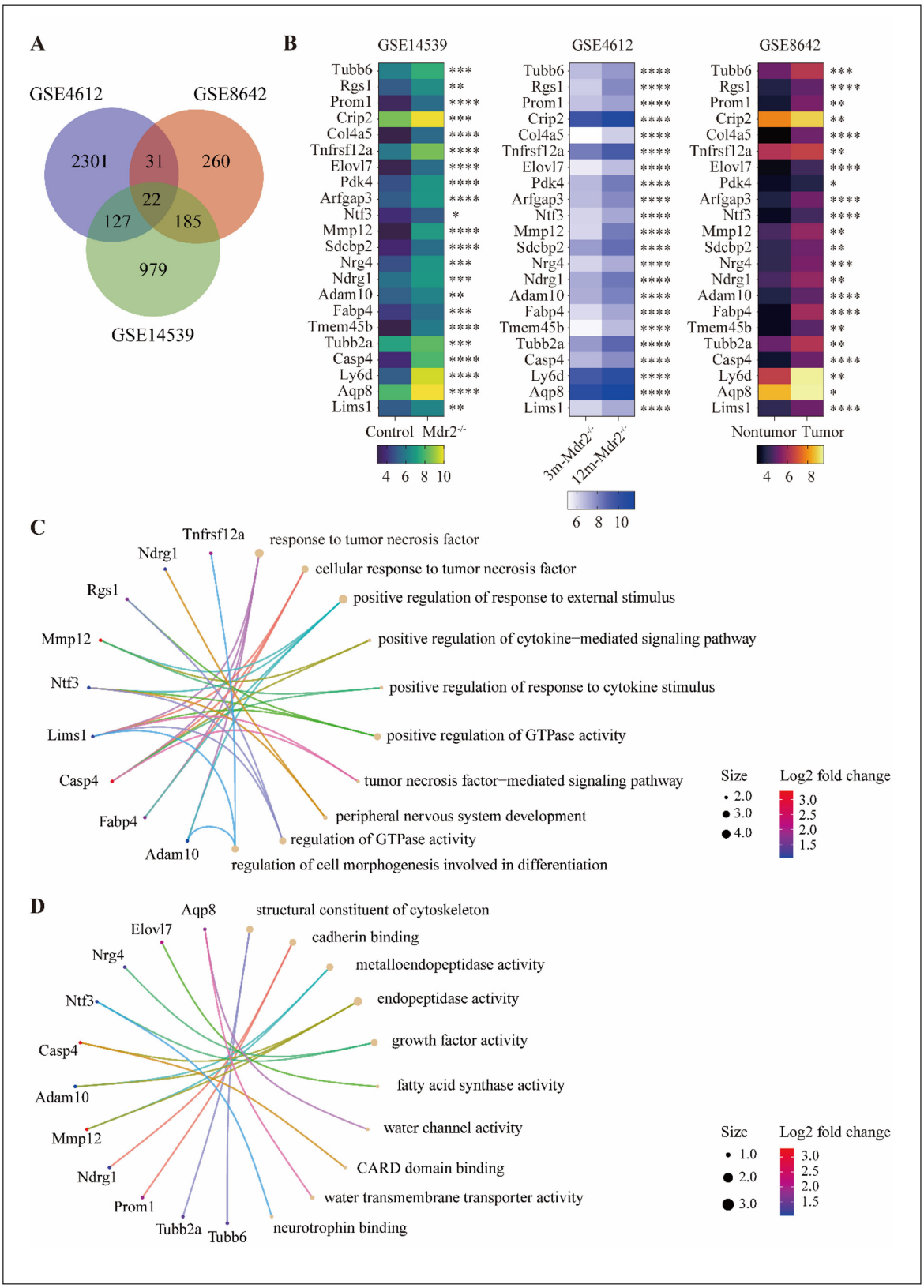

Figure 2. A total of 22 overlapped differentially expressed genes (DEGs) were identified in the GSE4612, GSE8642 and GSE14539 datasets. **A**, The gene expression comparison in these three Gene Expression Omnibus (GEO) series. **B**, The Gene Ontology (GO). **C**, biological process. **D**, molecular functions of these 22 overlapped DEGs.

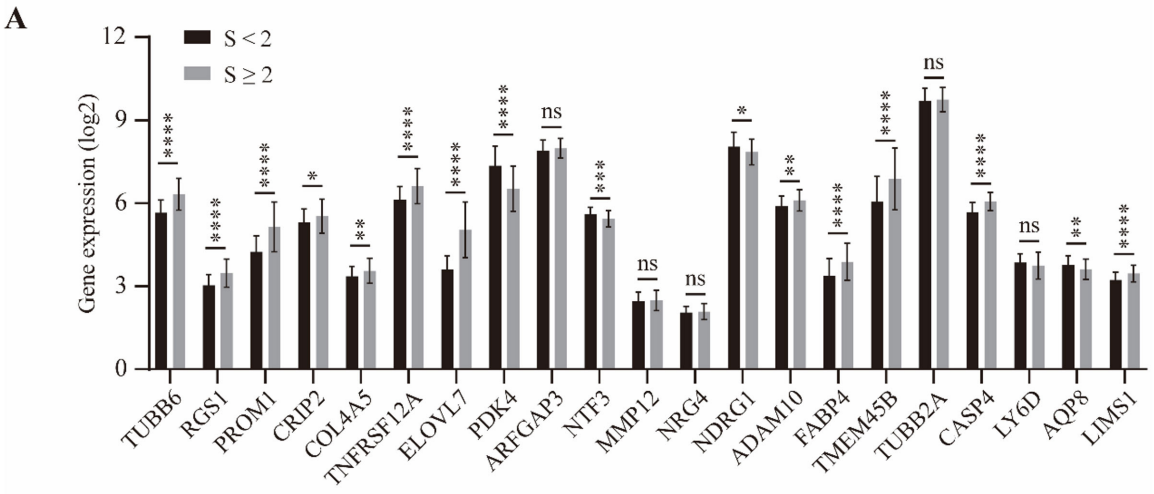

B

Univariate

Variables	Category	OR (95% CI)	*p* value
Age	Per increase 1 year	1.05 (1.02, 1.09)	0.002
TUBB6	Per increase 1 unit (log2)	13.9 (5.0, 38.5)	< 0.001
RGS1	Per increase 1 unit (log2)	8.3 (3.3, 21.0)	< 0.001
PROM1	Per increase 1 unit (log2)	5.3 (2.7, 10.3)	< 0.001
CRIP2	Per increase 1 unit (log2)	2.1 (1.1, 4.0)	0.03
COL4A5	Per increase 1 unit (log2)	3.5 (1.4, 8.8)	0.01
TNFRSF12A	Per increase 1 unit (log2)	4.9 (2.3, 10.4)	< 0.001
ELOVL7	Per increase 1 unit (log2)	13.8 (5.3, 36.1)	< 0.001
PDK4	Per increase 1 unit (log2)	0.22 (0.12, 0.42)	< 0.001
NTF3	Per increase 1 unit (log2)	0.09 (0.02, 0.36)	0.001
NDRG1	Per increase 1 unit (log2)	0.44 (0.21, 0.92)	0.029
ADAM10	Per increase 1 unit (log2)	4.5 (1.6, 12.40)	0.003
FABP4	Per increase 1 unit (log2)	3.8 (1.9, 7.6)	< 0.001
TMEM45B	Per increase 1 unit (log2)	2.2 (1.5, 3.3)	< 0.001
CASP4	Per increase 1 unit (log2)	24.3 (6.9, 85.7)	< 0.001
AQP8	Per increase 1 unit (log2)	0.25 (0.09, 0.74)	0.012
LIMS1	Per increase 1 unit (log2)	15.6 (3.9, 61.7)	< 0.001

C

Multivariate

Variables	Category	OR (95% CI)	*p* value
Age	Per increase 1 year	1.05 (0.98, 1.11)	0.165
TUBB6	Per increase 1 unit (log2)	1.5 (0.2, 14.5)	0.728
RGS1	Per increase 1 unit (log2)	0.5 (0.04, 4.9)	0.495
PROM1	Per increase 1 unit (log2)	1.5 (0.3, 6.8)	0.575
CRIP2	Per increase 1 unit (log2)	10.0 (0.7, 136.0)	0.083
COL4A5	Per increase 1 unit (log2)	0.4 (0.1, 2.7)	0.349
TNFRSF12A	Per increase 1 unit (log2)	0.4 (0.04, 3.5)	0.396
ELOVL7	Per increase 1 unit (log2)	11.8 (2.0, 69.2)	0.006
PDK4	Per increase 1 unit (log2)	0.4 (0.1, 1.4)	0.143
NTF3	Per increase 1 unit (log2)	0.2 (0.01, 2.6)	0.2
NDRG1	Per increase 1 unit (log2)	2.1 (0.5, 8.8)	0.292
ADAM10	Per increase 1 unit (log2)	0.5 (0.04, 6.2)	0.594
FABP4	Per increase 1 unit (log2)	1.2 (0.4, 3.8)	0.716
TMEM45B	Per increase 1 unit (log2)	1.03 (0.40, 2.5)	0.943
CASP4	Per increase 1 unit (log2)	1.4 (0.1, 24.4)	0.821
AQP8	Per increase 1 unit (log2)	0.8 (0.1, 12.3)	0.883
LIMS1	Per increase 1 unit (log2)	14.7 (0.6, 351.6)	0.097

Figure 3. **A**, The gene expression between fibrosis staging S < 2 and S ≥ 2 in the GSE84044. **B**, Univariate and (**C**), multivariate logistic regression analysis for predicting liver fibrosis S ≥ 2. **p* < 0.05, ***p* < 0.01, ****p* < 0.001, *****p* < 0.0001.

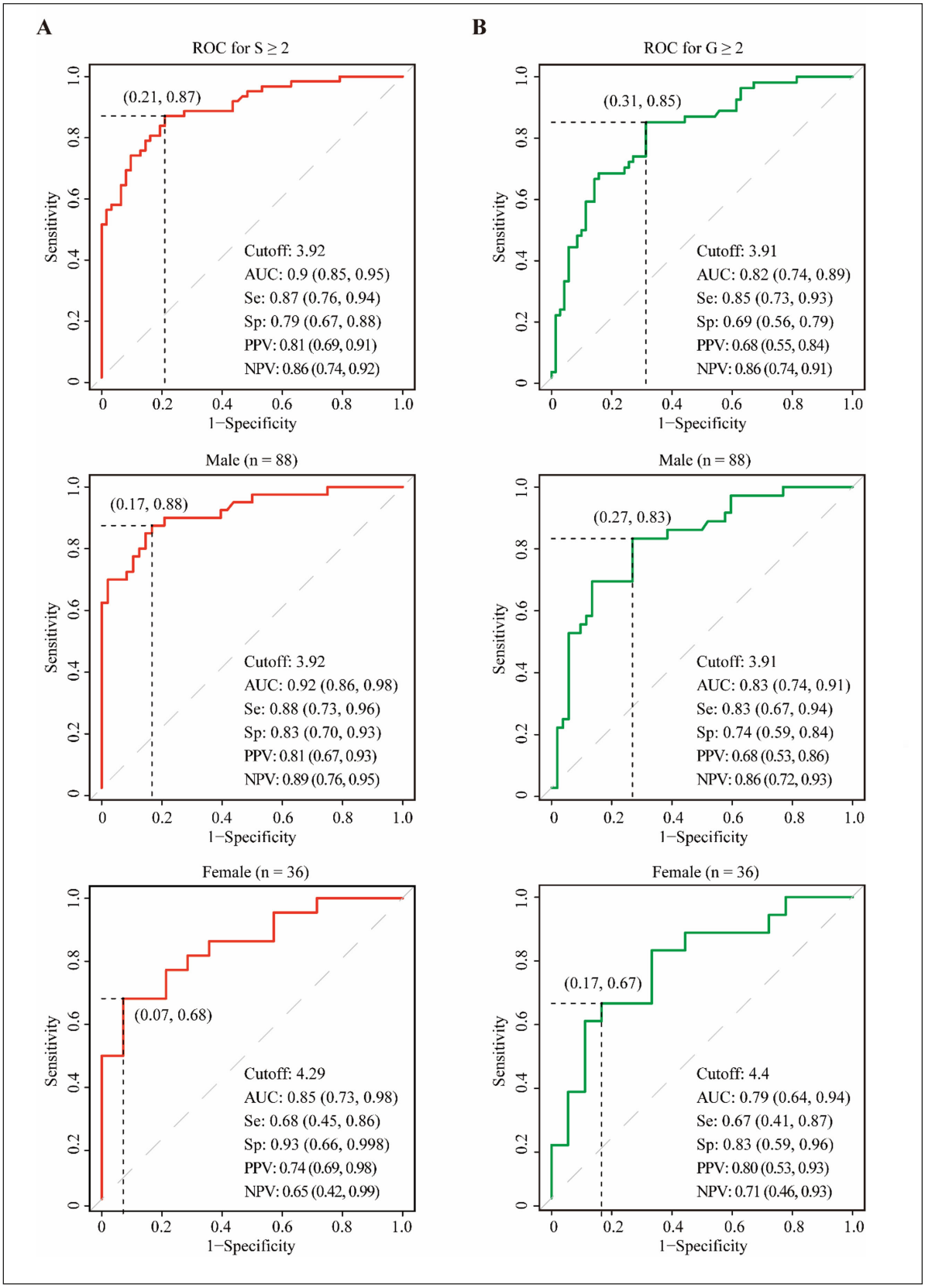

Figure 4. The receiver operating characteristic (ROC) curve of *ELOVL7* for liver fibrosis S ≥ 2 (**A**) and liver inflammation G ≥ 2 (**B**).

Subgroup analysis demonstrated that *ELOVL7* also showed outstanding predictive performance for liver fibrosis S ≥ 2 in both male and female (male patients: cutoff = 3.92, AUC = 0.92, 95% CI = 0.86 - 0.98; female patients: cutoff = 4.29, AUC = 0.85, 95% CI = 0.73 - 0.98; Figure 4A). Similarly, *ELOVL7* showed good predictive performance for liver inflammation G ≥ 2 [cutoff = 3.91, AUC = 0.82 (95% CI = 0.74 - 0.89), specificity = 0.85, sensitivity = 0.69, positive predictive value (PPV) = 0.68, and negative predictive value (NPV) = 0.86, Figure 4B], even in the male and female subgroups (male subgroup: cutoff = 3.91, AUC = 0.83, 95% CI = 0.74 - 0.91; female subgroup: cutoff = 4.4, AUC = 0.79, 95% CI = 0.64 - 0.94; Figure 4B).

DCA indicated that *ELOVL7*, with a threshold probability of 10% - 100%, showed good predictive value for liver fibrosis S ≥ 2 (Figure 5A). The true positive and false positive rates of *ELOVL7* for predicting liver fibrosis over a range of high-risk thresholds, as well as the clinical impact curve, are presented in Figure 5B. Similarly, *ELOVL7*, with a threshold probability of 10% - 75%, showed good predictive performance for liver inflammation G ≥ 2 (Figure 5C). The true positive and false positive rates of *ELOVL7* for predicting liver inflammation over a range of high-risk thresholds, as well as the clinical impact curve, are presented in Figure 5D.

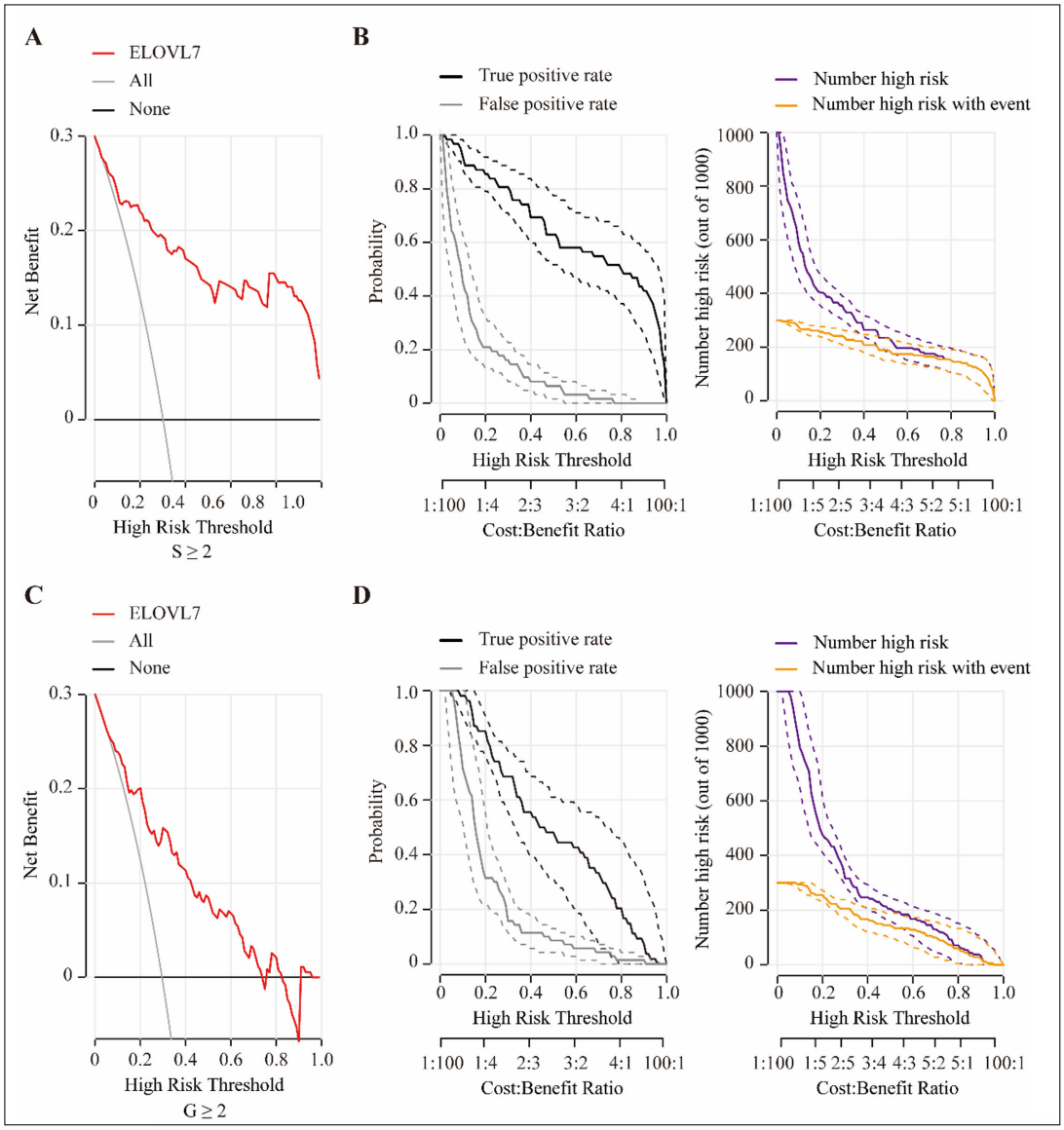

Figure 5. The Decision Curve Analysis (DCA) of *ELOVL7* for liver fibrosis S ≥ 2 (**A-B**), and liver inflammation G ≥ 2 (**C-D**).

ELOVL7 Expression in Liver Injury

Liver injury datasets were searched and downloaded from the GEO database. The identification framework and data algorithm were the same as noted above. Moreover, we conducted Spearman's Chi-square test to evaluate the correlation between *ELOVL7* expression and liver fibrosis staging in GSE84044[15]. As shown in Figure 6A, the *ELOVL7* level was positively correlated with the liver fibrosis staging ($r = 0.737$, $p < 0.001$, Figure 6A).

ELOVL7 expression was significantly upregulated in cirrhosis samples compared to normal liver or hepatitis samples in the GSE7741[33], GSE25097[34] and GSE103580[35] datasets ($p < 0.01$, Figure 6B). Additionally, our own RNA sequencing data indicated that *ELOVL7* levels were significantly higher in the patients with liver fibrosis $S \geq 2$ than in those with $S < 2$ ($p < 0.05$, GSE197112, Figure 6B).

ELOVL7 was significantly overexpressed in patients with HBV-associated acute liver failure compared with healthy individuals, patients with liver angioma ($p < 0.0001$, GSE14668[36] and GSE96851[37], Figure 6C) or CHB patients in the immune clearance stage ($p < 0.001$, GSE65359[38], Figure 6C). *ELOVL7* expression exhibited an increasing trend in CHB patient livers compared to normal livers ($p = 0.05$, GSE58208, Figure 6C). *ELOVL7* also showed an increasing trend in hepatitis C virus (HCV)-infected patients; unfortunately, no significant difference was found (Figure 6D).

ELOVL7 levels were significantly higher in nonalcoholic steatohepatitis (NASH) patients than in nonalcoholic fatty liver disease (NAFLD) patients or healthy subjects ($p < 0.05$, GSE49541[39], GSE58979[40] and GSE59045[40], Figure 6E). In C57BL/6 NASH mice fed a methionine- and choline-deficient (MCD) diet and a high-fat diet, *ELOVL7* expression was significantly upregulated compared to that in normal livers ($p < 0.0001$, GSE35961[41], Figure 6E). Similarly, *ELOVL7* was significantly overexpressed in the high-fat-diet-fed mice compared to normal-chow-diet-fed mice ($p < 0.0001$, GSE57425[42], Figure 6E).

In addition, *ELOVL7* levels were significantly increased in the liver injury models, including mice with bile duct ligation (BDL), mice with carbon tetrachloride (CCl_4) induction and C57BL6/N mice with paracetamol injection (all $p < 0.05$, Figure 6F). In addition, the injection of lipopolysaccharide (LPS) increased the levels of *ELOVL7*, but no significant difference was found ($p = 0.09$, GSE166488[43], Figure 6F).

In summary, *ELOVL7* is widely overexpressed in the setting of various types of liver injury, including HBV infection, non-alcoholic steatohepatitis (NASH), and some mouse models of liver damage.

Correlations Between ELOVL7 Expression and HSC Properties

To further investigate the roles of *ELOVL7* in the progression of liver fibrosis, we compared *ELOVL7* expression in different stages of HSCs. As shown in Figure 7A, *ELOVL7* was significantly upregulated in HSCs compared to liver stem/progenitor cells, hepatocytes, liver sinusoidal endothelial cells, and embryonic fibroblasts (all $p < 0.05$, GSE49995[44], GSE68000[45] and GSE106347[46], Figure 7A). *ELOVL7* was significantly overexpressed in activated HSCs compared to quiescent HSCs and reverted HSCs (all $p < 0.001$, GSE68000[45] and GSE68001[47], Figure 7A).

Since the transforming growth factor β (TGFβ) pathway is the core signaling pathway in the development of liver fibrosis and activation of HSCs, we determined the correlations between *ELOVL7* expression and *TGFβ1*, *TGFβ2*, and *TGFβ3* expression in the GSE84044 dataset. As shown in Figure 7B, *TGFβ2* was significantly upregulated in the high *ELOVL7* expression group ($p < 0.0001$, Figure 7B), and *TGFβ1* and *TGFβ3* expression exhibited an increasing trend according to *ELOVL7* upregulation ($p = 0.07$, Figure 7B). Spearman correlation analysis showed that *TGFβ1*, *TGFβ2*, and *TGFβ3* expression had positive correlations with *ELOVL7* expression ($r = 0.287$, $p = 0.001$; $r = 0.516$, $p < 0.001$ and $r = 0.211$, $p = 0.019$, respectively; Figure 7C). In addition, bone morphogenic protein 7 (*BMP7*) expression was negatively associated with *ELOVL7* expression in the GSE84044 dataset ($p < 0.001$, Figure 7D). *ELOVL7* expression was significantly increased in LX2 cells treated with recombinant human bone morphogenic protein 9 (*BMP9*) and in human umbilical vein endothelial cells (HUVECs) stimulated with *BMP9* (both $p < 0.05$, GSE104482 and GSE104684[48], Figure 7E).

In summary, *ELOVL7* expression is increased in activated HSCs and is involved in the activation of the TGFβ signaling pathway.

Enrichment of ELOVL7 Interacting Proteins

PPI analysis indicated significant interactions between ten proteins and *ELOVL7* in the STRING database (coefficient = 0.864, $p = 1.78 \times 10^{-8}$, Figure 8A). KEGG pathways such as biosynthesis of unsaturated fatty acids, fatty acid metabolism, fatty acid elongation, and metabolic pathways were enriched (Figure 8B). Reactome pathways such as fatty acid metabolism, fatty acyl-CoA biosynthesis, linoleic acid (LA) metabolism, synthesis of very long-chain fatty acid acyl-CoAs, and metabolism were enriched (Figure 8C).

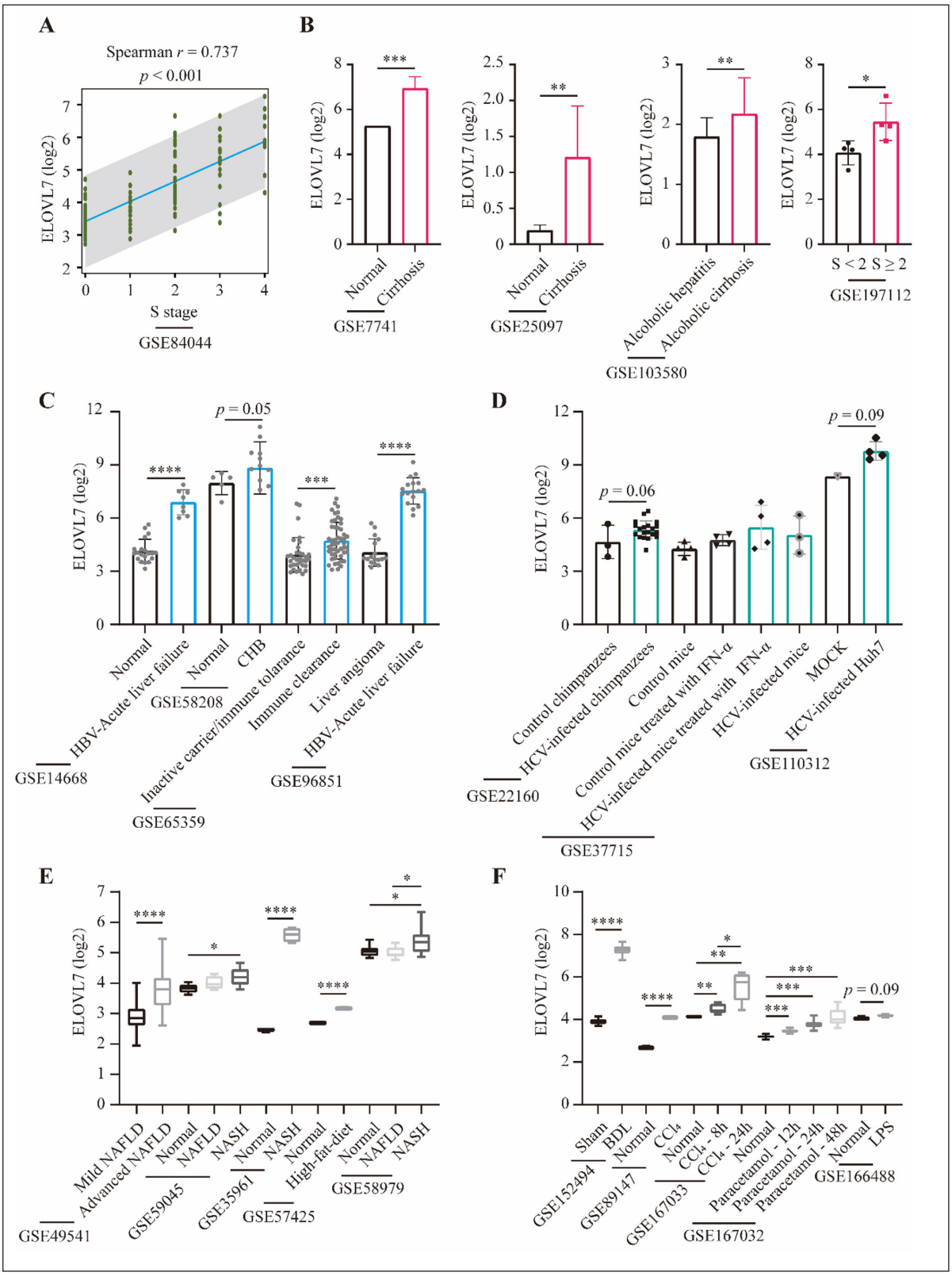

Figure 6. The correlation of *ELOVL7* and liver fibrosis staging (**A**); the *ELOVL7* expression in multiple liver injuries including cirrhosis (**B**), chronic hepatitis B (CHB) (**C**), hepatitis C virus (HCV) infection (**D**), non-alcoholic fatty liver disease (NAFLD) and non-alcoholic steatohepatitis (NASH) (**E**), and the liver injury models induced by bile duct ligation (BDL), carbon tetrachloride (CCl4), paracetamol injection and lipopolysaccharide (LPS) injection (**F**). *$p < 0.05$, **$p < 0.01$, ***$p < 0.001$, ****$p < 0.0001$.

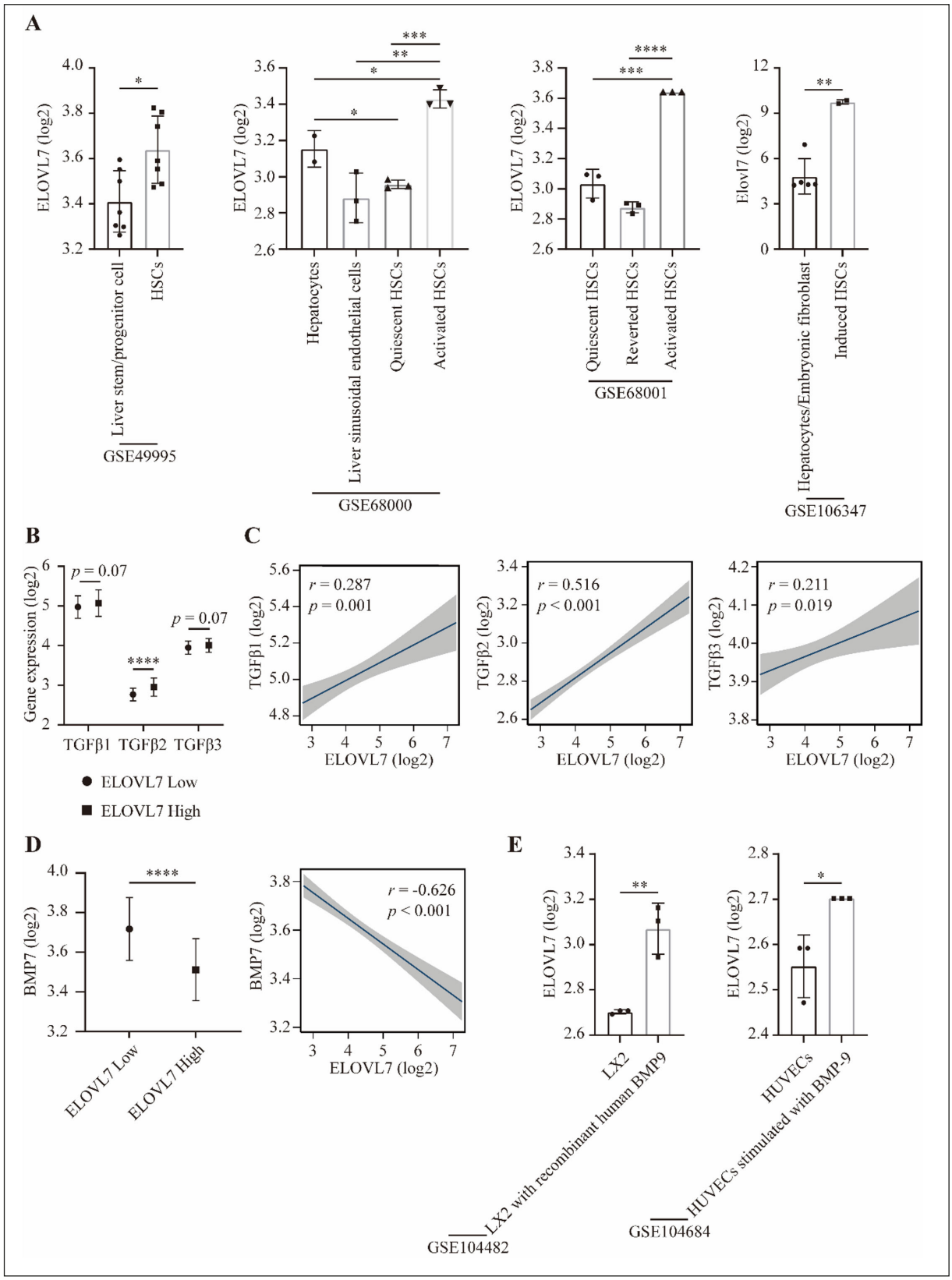

Figure 7. The *ELOVL7* expression in different status of hepatic stellate cells (HSCs) (**A**), and the correlation between *ELOVL7* and biomarkers in the transforming growth factor β (TGFβ) pathway including *TGFβ1*, *TGFβ2*, *TGFβ3*, bone morphogenic protein 7 (*BMP7*) and bone morphogenic protein 9 (*BMP9*) (**B-E**). *$p < 0.05$, **$p < 0.01$, ***$p < 0.001$, ****$p < 0.0001$.

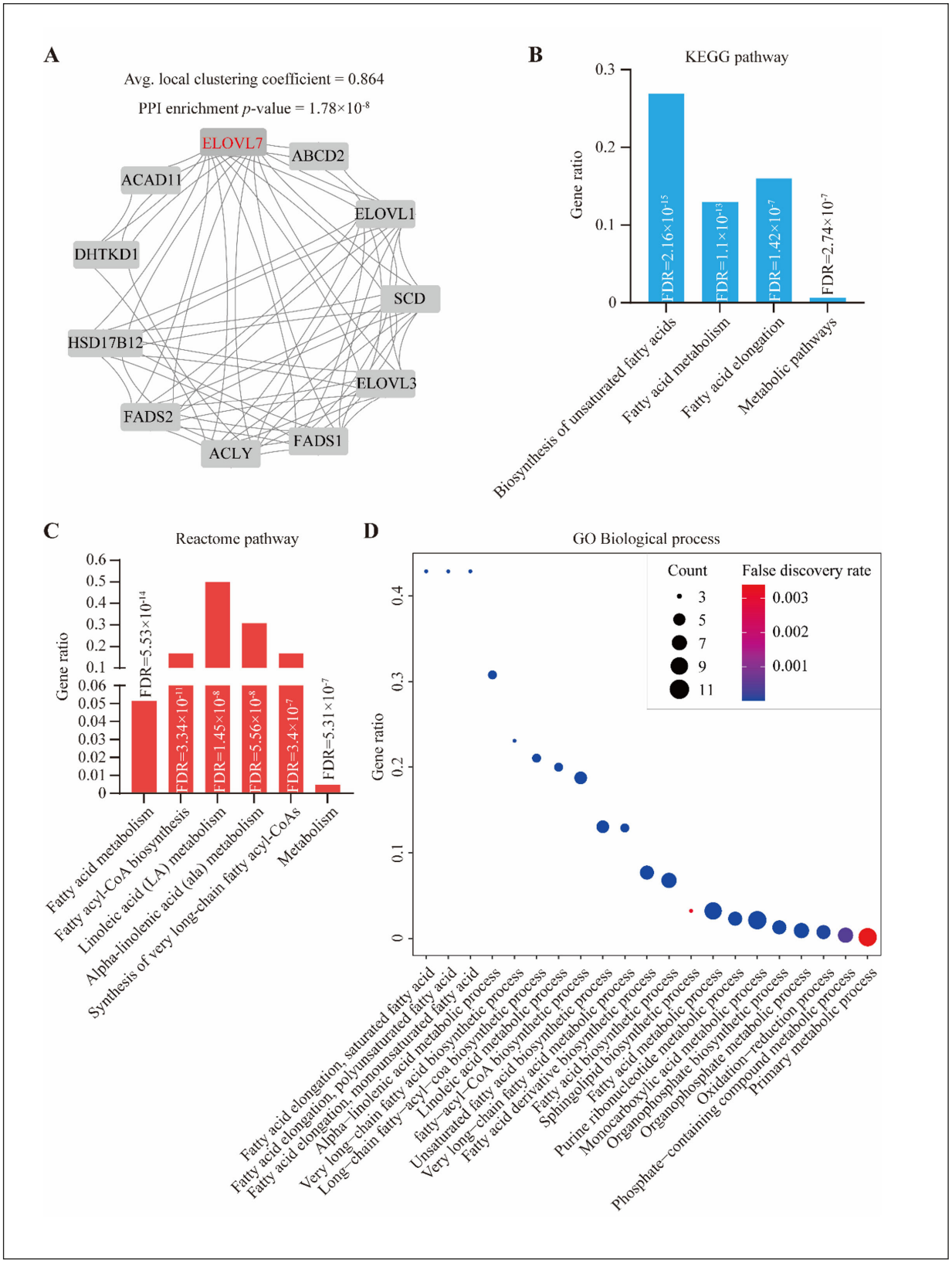

Figure 8. The protein-protein interaction (PPI) of *ELOVL7* (**A**), and the Kyoto Encyclopedia of Genes and Genomes (KEGG) pathway (**B**), Reactome pathway (**C**), and Gene Ontology (GO) biological process (**D**) enrichments of the *ELOVL7* interacted proteins.

GO enrichment analysis also confirmed that these interacting proteins were involved mainly in the biological process of fatty acid synthesis and metabolism (Figure 8D).

Discussion

Ablation of *Mdr2* leads to intrahepatic bile accumulation and cholestatic liver fibrosis[19,49]. *Mdr2* is the rodent homolog of the human Mdr3 protein, and emerging evidence indicates that genetic mutations in the *ABCC4* gene, encoding *Mdr3*, are associated with cholestasis and cirrhosis[50-52]. However, the relationships between genes with expression alterations, induced by *Mdr2* deletion and noncholestatic cirrhosis in humans, remain uncertain[8]. In this study, we found that the genes with expression alterations induced by knockout of *Mdr2* were involved mainly in the biological processes of response to cytokines and cell differentiation. Among these altered genes, *ELOVL7* was identified as a promising predictor of advanced liver fibrosis and liver inflammation.

Our enrichment analysis indicated that *ELOVL7* interacted with genes involved in fatty acid synthesis and metabolism. In humans, *ELOVL7* participates in the synthesis of long-chain fatty acids, elongates saturated and monosaturated fatty acids and assists with lipid formation[53-55]. It exhibits high activity toward acyl-CoAs with C18 carbon chain length. Previous studies[56] have showed that *ELOVL7* is involved in prostate cancer cell viability and survival by regulating the levels of saturated very-long-chain fatty acids and their derivatives. Human cytomegalovirus infection-induced *ELOVL7* upregulation is dependent on mammalian target of rapamycin (*mTOR*) and sterol regulatory element-binding transcription factor 1 (*SREBP1*)[54]. The α-linolenic acid was found to enhance *ELOVL7* promoter activation and result in the accumulation of cellular fat, suggesting that *ELOVL7* is involved in fatty acid metabolism in bovine mammary epithelial cells[57]. *ELOVL7* mRNA is expressed at relatively low levels in normal livers[58]. Notably, our data revealed that the level of *ELOVL7* was increased in various types of liver injury, advanced liver fibrosis and cirrhosis. Non-alcoholic fatty liver disease (NAFLD), which is characterized by an imbalance in fatty acid synthesis and lipid metabolism, can regularly progress to NASH, which increases the risk of liver fibrosis and cirrhosis[59]. Dysfunction of fatty acid synthesis and metabolism leads to increased levels of hepatic fatty acids, resulting in multiple liver insults, for instance, mitochondrial dysfunction, endoplasmic reticulum stress, and the release of inflammatory cytokines, which trigger signaling cascades related to inflammation, cell death, and liver fibrosis[60,61]. According to some studies[57-61] and our results, we assumed that *ELOVL7* can promote liver fibrosis progression *via* fatty acid-related mechanisms.

HSCs are the core factors in liver fibrosis development[62]. Our data demonstrated that *ELOVL7* activity was elevated in activated HSCs compared to normal liver cells and quiescent HSCs. HSCs are the main fibrogenic cells in the damaged liver, accounting for most of the proliferative, contractile, and fibrogenic myofibroblasts that are involved in the process of liver fibrosis[3,62]. During the activation of quiescent HSCs, the content of lipid droplets changes, and the content of ribonucleic acid decreases but that of triacylglycerols (TAGs) increases; the increase of TAGs is likely dependent on the modulated expression of diacylglycerol O-cyltransferase-1 and adipose triglyceride lipase, both of which are involved in the synthesis and breakdown of TAGs[63,64]. Finally, stabilized ribonucleic acid is released from lipid droplets for the catabolism and β-oxidation of fatty acids[65]. Hence, as a regulator of fatty acid synthesis and metabolism, *ELOVL7* upregulation during HSC activation is expected to contribute to the progression of liver fibrosis.

Multiple genes and multiple factors are involved in the activation of HSCs, and the related signaling pathways may constitute potential therapeutic targets. Among these pathways, TGFβ signaling is generally recognized to participate in the development of liver fibrosis[66]. In our analysis, we found that *ELOVL7* expression was positively correlated with *TGFβ1*, *TGFβ2*, and *TGFβ3* expression and was especially upregulated in livers with high *TGFβ2* high expression. On the other hand, *ELOVL7* expression was negatively correlated with *BMP7* expression and was upregulated in *BMP9*-treated cells. Current publications have indicated that *TGFβ2* can induce expression of a number of fibrotic genes in cholangiocytes and HSCs[67]. *BMP7*, a member of the TGFβ superfamily, can decrease the expression of collagen 1A2 and α-smooth muscle actin (α-SMA), trigger the expression of inhibitors of differentiation 2, and inhibit the expression of *TGFβ1* and the epidermal growth factor receptor, resulting in alleviation of liver fibrosis[68,69]. *BMP9*, also called growth differentiation factor 2 (*GDF2*), is a member of the TGFβ superfamily and is involved in the

promotion of liver fibrosis progression[70,71]. Considering the previous studies[66-71] and our results, we hypothesized that *ELOVL7* might induce the activation of the TGFβ signaling pathway during the development of liver fibrosis.

Limitations

This study has some limitations. First, our analysis was based on public datasets, and the clinical characteristics of the included patients were incomplete; for instance, liver function parameters and virological markers were not obtained and adjusted for, which might result in biases regarding the predictive power of *ELOVL7* for liver fibrosis. Second, *ELOVL7* protein expression in different liver fibrosis stages was not investigated, and the correlation and consistency of *ELOVL7* levels between liver tissues and peripheral blood mononuclear cells (PBMCs) have not been investigated, which currently limits the clinical application of this candidate. Third, the mechanisms of *ELOVL7* in the development of liver fibrosis were discussed superficially in this study. Considering the complicated mechanisms of liver fibrosis, the genetic, epigenetic and metabolic aspects of the role of *ELOVL7* in liver fibrosis progression should be investigated in depth.

Conclusions

ELOVL7 can accurately predict advanced liver fibrosis and be involved mainly in the activation of HSCs and the TGFβ signaling pathway. This candidate is expected to be a diagnostic and therapeutic target in liver fibrosis. Future research should focus on the relationship between the expression levels of *ELOVL7* in PBMCs and the severity of liver fibrosis to verify the possibility of its clinical application.

Conflicts of Interest

The authors declare no conflicts of interest in this work.

Ethics Approval

The protocol of this secondary analysis was reviewed and approved by the Ethics Committee of Beijing Tian Tan Hospital, Capital Medical University.

Informed Consent

Written informed consent was obtained from all participants.

Availability of Data and Materials

The datasets used in the current study are available in the NCBI Gene Expression Omnibus (GEO, https://www.ncbi.nlm.nih.gov/geo/). All the datasets are available from Dr. Qian Dong upon reasonable request.

Authors' Contributions

Qian Dong and Zong-Guo Yang conceived and designed the study. Wen-Ming Wang wrote the manuscript. Qian Dong revised the manuscript. Wen-Ming Wang, Qian Dong, Cheng Liu, and Zong-Guo Yang analyzed and interpreted the data. All authors read and approved the final manuscript.

Funding

This work was supported by the Shanghai Municipal Health Commission (grant number 2020LZ001). The funders had no role in the study design, data collection and analysis, decision to publish, or manuscript preparation.

ORCID ID

Wen-Ming Wang: 0000-0002-0610-6282
Zong-Guo Yang: 0000-0002-6623-4841
Cheng Liu: 0000-0002-8741-6169
Qian Dong: 0000-0003-0588-2498

References

1) Henderson NC, Rieder F, Wynn TA. Fibrosis: from mechanisms to medicines. Nature 2020; 587: 555-566.
2) Rockey DC, Bell PD, Hill JA. Fibrosis--a common pathway to organ injury and failure. N Engl J Med 2015; 372: 1138-1149.
3) Delgado ME, Cardenas BI, Farran N, Fernandez M. Metabolic Reprogramming of Liver Fibrosis. Cells 2021; 10: 3604.
4) Wang FD, Zhou J, Chen EQ. Molecular Mechanisms and Potential New Therapeutic Drugs for Liver Fibrosis. Front Pharmacol 2022; 13: 787748.
5) Kaur N, Goyal G, Garg R, Tapasvi C, Chawla S, Kaur R. Potential role of noninvasive biomarkers during liver fibrosis. World J Hepatol 2021; 13: 1919-1935.
6) Brenner DA. Molecular pathogenesis of liver fibrosis. Trans Am Clin Climatol Assoc 2009; 120: 361-368.
7) Zhou WC, Zhang QB, Qiao L. Pathogenesis of liver cirrhosis. World J Gastroenterol 2014; 20: 7312-7324.
8) Li M, Ping J, Xu LM. [Application of Mdr2 gene knockout mice in liver disease research]. Zhonghua Gan Zang Bing Za Zhi 2021; 29: 585-590.
9) Popov Y, Patsenker E, Fickert P, Trauner M, Schuppan D. Mdr2 (Abcb4)-/- mice spontaneously develop severe biliary fibrosis via massive dysregulation of pro- and antifibrogenic genes. J Hepatol 2005; 43: 1045-1054.

10) Fuchs M, Stange EF. Cholesterol and cholestasis: a lesson from the Mdr2 (-/-) mouse. J Hepatol 2001; 34: 339-341.
11) Gonzales E, Davit-Spraul A, Baussan C, Buffet C, Maurice M, Jacquemin E. Liver diseases related to MDR3 (ABCB4) gene deficiency. Front Biosci (Landmark Ed) 2009; 14: 4242-4256.
12) Wu H, Chen C, Ziani S, Nelson LJ,Ávila MA, Nevzorova YA, Cubero FJ. Fibrotic Events in the Progression of Cholestatic Liver Disease. Cells 2021; 10: 1107.
13) Fickert P, Fuchsbichler A, Wagner M, Zollner G, Kaser A, Tilg H, Krause R, Lammert F, Langner C, Zatloukal K, Marschall HU, Denk H, Trauner M. Regurgitation of bile acids from leaky bile ducts causes sclerosing cholangitis in Mdr2 (Abcb4) knockout mice. Gastroenterology 2004; 127: 261-274.
14) Wang WM, Zhang WS, Yang ZG. Vimentin (VIM) predicts advanced liver fibrosis in chronic hepatitis B patients: A random forest-derived analysis. Eur Rev Med Pharmacol Sci 2022; 26: 5164-5177.
15) Wang M, Gong Q, Zhang J, Chen L, Zhang Z, Lu L, Yu D, Han Y, Zhang D, Chen P, Zhang X, Yuan Z, Huang J, Zhang X. Characterization of gene expression profiles in HBV-related liver fibrosis patients and identification of ITGBL1 as a key regulator of fibrogenesis. Sci Rep 2017; 7: 43446.
16) Barrett T, Wilhite SE, Ledoux P, Evangelista C, Kim IF, Tomashevsky M, Marshall KA, Phillippy KH, Sherman PM, Holko M, Yefanov A, Lee H, Zhang N, Robertson CL, Serova N, Davis S, Soboleva A. NCBI GEO: archive for functional genomics data sets--update. Nucleic Acids Res 2013; 41: D991-D995.
17) Wilhite SE, Barrett T. Strategies to explore functional genomics data sets in NCBI's GEO database. Methods Mol Biol 2012; 802: 41-53.
18) Katzenellenbogen M, Pappo O, Barash H, Klopstock N, Mizrahi L, Olam D, Jacob-Hirsch J, Amariglio N, Rechavi G, Mitchell LA, Kohen R, Domany E, Galun E, Goldenberg D. Multiple adaptive mechanisms to chronic liver disease revealed at early stages of liver carcinogenesis in the Mdr2-knockout mice. Cancer Res 2006; 66: 4001-4010.
19) Katzenellenbogen M, Mizrahi L, Pappo O, Klopstock N, Olam D, Jacob-Hirsch J, Amariglio N, Rechavi G, Domany E, Galun E, Goldenberg D. Molecular mechanisms of liver carcinogenesis in the mdr2-knockout mice. Mol Cancer Res 2007; 5: 1159-1170.
20) Barash H, R Gross E, Edrei Y, Ella E, Israel A, Cohen I, Corchia N, Ben-Moshe T, Pappo O, Pikarsky E, Goldenberg D, Shiloh Y, Galun E, Abramovitch R. Accelerated carcinogenesis following liver regeneration is associated with chronic inflammation-induced double-strand DNA breaks. Proc Natl Acad Sci U S A 2010; 107: 2207-2212.
21) Zhang Y, Lu W, Chen X, Cao Y, Yang Z. A Bioinformatic Analysis of Correlations between Polymeric Immunoglobulin Receptor (PIGR) and Liver Fibrosis Progression. Biomed Res Int 2021; 2021: 5541780.
22) Liaw YF, Leung N, Kao JH, Piratvisuth T, Gane E, Han KH, Guan R, Lau GKK, Locarnini S, Chronic Hepatitis B Guideline Working Party of the Asian-Pacific Association for the Study of the Liver. Asian-Pacific consensus statement on the management of chronic hepatitis B: a 2008 update. Hepatol Int 2008; 2: 263-283.
23) Desmet VJ, Gerber M, Hoofnagle JH, Manns M, Scheuer PJ. Classification of chronic hepatitis: diagnosis, grading and staging. Hepatology 1994; 19: 1513-1520.
24) Goodman ZD. Grading and staging systems for inflammation and fibrosis in chronic liver diseases. J Hepatol 2007; 47: 598-607.
25) Gautier L, Cope L, Bolstad BM, Irizarry RA. affy--analysis of Affymetrix GeneChip data at the probe level. Bioinformatics 2004; 20: 307-315.
26) Ritchie ME, Phipson B, Wu D, Hu Y, Law CW, Shi W, Smyth GK. limma powers differential expression analyses for RNA-sequencing and microarray studies. Nucleic Acids Res 2015; 43: e47.
27) Dong X, Lin L, Zhang R, Zhao Y, Christiani DC, Wei Y, Chen F. TOBMI: trans-omics block missing data imputation using a k-nearest neighbor weighted approach. Bioinformatics 2019; 35: 1278-1283.
28) Szklarczyk D, Gable AL, Lyon D, Junge A, Wyder S, Huerta-Cepas J, Simonovic M, Doncheva NT, Morris JH, Bork P, Jensen LJ, von Mering C. STRING v11: protein-protein association networks with increased coverage, supporting functional discovery in genome-wide experimental datasets. Nucleic Acids Res 2019; 47: D607-D613.
29) Szklarczyk D, Gable AL, Nastou KC, Lyon D, Kirsch R, Pyysalo S, Doncheva NT, Legeay M, Fang T, Bork P, Jensen LJ, von Mering C. The STRING database in 2021: customizable protein-protein networks, and functional characterization of user-uploaded gene/measurement sets. Nucleic Acids Res 2021; 49: D605-D612.
30) López-Ratón M, Rodríguez-Álvarez MX, Cadarso-Suárez C, Gude-Sampedro F. OptimalCutpoints: An R Package for Selecting Optimal Cutpoints in Diagnostic Tests. J Stat Softw 2014; 61: 1-36.
31) Kerr KF, Brown MD, Zhu K, Janes H. Assessing the Clinical Impact of Risk Prediction Models With Decision Curves: Guidance for Correct Interpretation and Appropriate Use. J Clin Oncol 2016; 34: 2534-2540.
32) Vickers AJ, Elkin EB. Decision curve analysis: a novel method for evaluating prediction models. Med Decis Making 2006; 26: 565-574.
33) Khalid SS, Hamid S, Siddiqui AA, Qureshi A, Qureshi N. Gene profiling of early and advanced liver disease in chronic hepatitis C patients. Hepatol Int 2011; 5: 782-788.
34) Ivanovska I, Zhang C, Liu AM, Wong KF, Lee NP, Lewis P, Philippar U, Bansal D, Buser C, Scott M, Mao M, Poon RT, Fan ST, Cleary MA, Luk JM, Dai H. Gene signatures derived from a c-MET-driven liver cancer mouse model predict survival of patients with hepatocellular carcinoma. PLoS One 2011; 6: e24582.

35) Trépo E, Goossens N, Fujiwara N, Song WM, Colaprico A, Marot A, Spahr L, Demetter P, Sempoux C, Im GY, Saldarriaga J, Gustot T, Devière J, Thung SN, Minsart C, Sersté T, Bontempi G, Abdelrahman K, Henrion J, Degré D, Lucidi V, Rubbia-Brandt L, Nair VD, Moreno C, Deltenre P, Hoshida Y, Franchimont D. Combination of Gene Expression Signature and Model for End-Stage Liver Disease Score Predicts Survival of Patients With Severe Alcoholic Hepatitis. Gastroenterology 2018; 154: 965-975.
36) Farci P, Diaz G, Chen Z, Govindarajan S, Tice A, Agulto L, Pittaluga S, Boon D, Yu C, Engle RE, Haas M, Simon R, Purcell RH, Zamboni F. B cell gene signature with massive intrahepatic production of antibodies to hepatitis B core antigen in hepatitis B virus-associated acute liver failure. Proc Natl Acad Sci U S A 2010; 107: 8766-8771.
37) Chen Z, Diaz G, Pollicino T, Zhao H, Engle RE, Schuck P, Shen CH, Zamboni F, Long Z, Kabat J, De Battista D, Bock KW, Moore IN, Wollenberg K, Soto C, Govindarajan S, Kwong PD, Kleiner DE, Purcell RH, Farci P. Role of humoral immunity against hepatitis B virus core antigen in the pathogenesis of acute liver failure. Proc Natl Acad Sci U S A 2018; 115: E11369-E11378.
38) Liu H, Li F, Zhang X, Yu J, Wang J, Jia J, Yu X, Shen Z, Yuan Z, Zhang X, Zhang Z, Zhang X, Lu L, Li H, Lu M, Zhang J. Differentially Expressed Intrahepatic Genes Contribute to Control of Hepatitis B Virus Replication in the Inactive Carrier Phase. J Infect Dis 2018; 217: 1044-1054.
39) Murphy SK, Yang H, Moylan CA, Pang H, Dellinger A, Abdelmalek MF, Garrett ME, Ashley-Koch A, Suzuki A, Tillmann HL, Hauser MA, Diehl AM. Relationship between methylome and transcriptome in patients with nonalcoholic fatty liver disease. Gastroenterology 2013; 145: 1076-1087.
40) du Plessis J, van Pelt J, Korf H, Mathieu C, van der Schueren B, Lannoo M, Oyen T, Topal B, Fetter G, Nayler S, van der Merwe T, Windmolders P, Van Gaal L, Verrijken A, Hubens G, Gericke M, Cassiman D, Francque S, Nevens F, van der Merwe S. Association of Adipose Tissue Inflammation With Histologic Severity of Nonalcoholic Fatty Liver Disease. Gastroenterology 2015; 149: 635-648.e14.
41) Kita Y, Takamura T, Misu H, Ota T, Kurita S, Takeshita Y, Uno M, Matsuzawa-Nagata N, Kato K, Ando H, Fujimura A, Hayashi K, Kimura T, Ni Y, Otoda T, Miyamoto K, Zen Y, Nakanuma Y, Kaneko S. Metformin prevents and reverses inflammation in a non-diabetic mouse model of nonalcoholic steatohepatitis. PLoS One 2012; 7: e43056.
42) Lu Y, Liu X, Jiao Y, Xiong X, Wang E, Wang X, Zhang Z, Zhang H, Pan L, Guan Y, Cai D, Ning G, Li X. Periostin promotes liver steatosis and hypertriglyceridemia through downregulation of PPARα. J Clin Invest 2014; 124: 3501-3513.
43) Holland CH, Ramirez Flores RO, Myllys M, Hassan R, Edlund K, Hofmann U, Marchan R, Cadenas C, Reinders J, Hoehme S, Seddek AL, Dooley S, Keitel V, Godoy P, Begher-Tibbe B, Trautwein C, Rupp C, Mueller S, Longerich T, Hengstler JG, Saez-Rodriguez J, Ghallab A. Transcriptomic Cross-Species Analysis of Chronic Liver Disease Reveals Consistent Regulation Between Humans and Mice. Hepatol Commun 2022; 6: 161-177.
44) Berardis S, Lombard C, Evraerts J, El Taghdouini A, Rosseels V, Sancho-Bru P, Lozano JJ, van Grunsven L, Sokal E, Najimi M. Gene expression profiling and secretome analysis differentiate adult-derived human liver stem/progenitor cells and human hepatic stellate cells. PLoS One 2014; 9: e86137.
45) El Taghdouini A, Sørensen AL, Reiner AH, Coll M, Verhulst S, Mannaerts I, Øie CI, Smedsrød B, Najimi M, Sokal E, Luttun A, Sancho-Bru P, Collas P, van Grunsven LA. Genome-wide analysis of DNA methylation and gene expression patterns in purified, uncultured human liver cells and activated hepatic stellate cells. Oncotarget 2015; 6: 26729-26745.
46) Park MR, Wong MS, Araúzo-Bravo MJ, Lee H, Nam D, Park SY, Seo HD, Lee SM, Zeilhofer HF, Zaehres H, Schöler HR, Kim JB. Oct4 and Hnf4α-induced hepatic stem cells ameliorate chronic liver injury in liver fibrosis model. PLoS One 2019; 14: e0221085.
47) El Taghdouini A, Najimi M, Sancho-Bru P, Sokal E, van Grunsven LA. In vitro reversion of activated primary human hepatic stellate cells. Fibrogenesis Tissue Repair 2015; 8: 14.
48) Morikawa M, Mitani Y, Holmborn K, Kato T, Koinuma D, Maruyama J, Vasilaki E, Sawada H, Kobayashi M, Ozawa T, Morishita Y, Bessho Y, Maeda S, Ledin J, Aburatani H, Kageyama R, Maruyama K, Heldin CH, Miyazono K. The ALK-1/SMAD/ATOH8 axis attenuates hypoxic responses and protects against the development of pulmonary arterial hypertension. Sci Signal 2019; 12: eaay4430.
49) Smit JJ, Schinkel AH, Oude Elferink RP, Groen AK, Wagenaar E, van Deemter L, Mol CA, Ottenhoff R, van der Lugt NM, van Roon MA, van der Valk MA, Offerhaus GJ, Berns AJ, Borst P. Homozygous disruption of the murine mdr2 P-glycoprotein gene leads to a complete absence of phospholipid from bile and to liver disease. Cell 1993; 75: 451-462.
50) Jacquemin E, De Vree JM, Cresteil D, Sokal EM, Sturm E, Dumont M, Scheffer GL, Paul M, Burdelski M, Bosma PJ, Bernard O, Hadchouel M, Elferink RP. The wide spectrum of multidrug resistance 3 deficiency: from neonatal cholestasis to cirrhosis of adulthood. Gastroenterology 2001; 120: 1448-1458.
51) Rosmorduc O, Hermelin B, Poupon R. MDR3 gene defect in adults with symptomatic intrahepatic and gallbladder cholesterol cholelithiasis. Gastroenterology 2001; 120: 1459-1467.
52) Petrescu AD, Grant S, Williams E, Frampton G, Reinhart EH, Nguyen A, An S, McMillin M, DeMorrow S. Ghrelin reverses ductular reaction and hepatic fibrosis in a rodent model of cholestasis. Sci Rep 2020; 10: 16024.
53) Naganuma T, Sato Y, Sassa T, Ohno Y, Kihara A. Biochemical characterization of the very long-chain fatty acid elongase ELOVL7. FEBS Lett 2011; 585: 3337-3341.

54) Purdy JG, Shenk T, Rabinowitz JD. Fatty acid elongase 7 catalyzes lipidome remodeling essential for human cytomegalovirus replication. Cell Rep 2015; 10: 1375-1385.
55) Kihara A. Very long-chain fatty acids: elongation, physiology and related disorders. J Biochem 2012; 152: 387-395.
56) Tamura K, Makino A, Hullin-Matsuda F, Kobayashi T, Furihata M, Chung S, Ashida S, Miki T, Fujioka T, Shuin T, Nakamura Y, Nakagawa H. Novel lipogenic enzyme ELOVL7 is involved in prostate cancer growth through saturated long-chain fatty acid metabolism. Cancer Res 2009; 69: 8133-8140.
57) Chen S, Hu Z, He H, Liu X. Fatty acid elongase7 is regulated via SP1 and is involved in lipid accumulation in bovine mammary epithelial cells. J Cell Physiol 2018; 233: 4715-4725.
58) Ohno Y, Suto S, Yamanaka M, Mizutani Y, Mitsutake S, Igarashi Y, Sassa T, Kihara A. ELOVL1 production of C24 acyl-CoAs is linked to C24 sphingolipid synthesis. Proc Natl Acad Sci U S A 2010; 107: 18439-18444.
59) Sunami Y. NASH, Fibrosis and Hepatocellular Carcinoma: Lipid Synthesis and Glutamine/Acetate Signaling. Int J Mol Sci 2020; 21: 6799.
60) Bessone F, Razori MV, Roma MG. Molecular pathways of nonalcoholic fatty liver disease development and progression. Cell Mol Life Sci 2019; 76: 99-128.
61) Pittala S, Krelin Y, Kuperman Y, Shoshan-Barmatz V. A Mitochondrial VDAC1-Based Peptide Greatly Suppresses Steatosis and NASH-Associated Pathologies in a Mouse Model. Mol Ther 2019; 27: 1848-1862.
62) Friedman SL. Hepatic stellate cells: protean, multifunctional, and enigmatic cells of the liver. Physiol Rev 2008; 88: 125-172.
63) Molenaar MR, Vaandrager AB, Helms JB. Some Lipid Droplets Are More Equal Than Others: Different Metabolic Lipid Droplet Pools in Hepatic Stellate Cells. Lipid Insights 2017; 10: 1178635317747281.
64) Tuohetahuntila M, Molenaar MR, Spee B, Brouwers JF, Wubbolts R, Houweling M, Yan C, Du H, VanderVen BC, Vaandrager AB, Helms JB. Lysosome-mediated degradation of a distinct pool of lipid droplets during hepatic stellate cell activation. J Biol Chem 2017; 292: 12436-12448.
65) Saeed A, Dullaart RPF, Schreuder T, Blokzijl H, Faber KN. Disturbed Vitamin A Metabolism in Non-Alcoholic Fatty Liver Disease (NAFLD). Nutrients 2017; 10: 29.
66) Zhao J, Cheng J. [Research progress of signaling pathways in liver fibrosis]. Zhonghua Gan Zang Bing Za Zhi 2019; 27: 403-406.
67) Dropmann A, Dooley S, Dewidar B, Hammad S, Dediulia T, Werle J, Hartwig V, Ghafoory S, Woelfl S, Korhonen H, Janicot M, Wosikowski K, Itzel T, Teufel A, Schuppan D, Stojanovic A, Cerwenka A, Nittka S, Piiper A, Gaiser T, Beraza N, Milkiewicz M, Milkiewicz P, Brain JG, Jones DEJ, Weiss TS, Zanger UM, Ebert M, Meindl-Beinker NM. TGF-β2 silencing to target biliary-derived liver diseases. Gut 2020; 69: 1677-1690.
68) Kinoshita K, Iimuro Y, Otogawa K, Saika S, Inagaki Y, Nakajima Y, Kawada N, Fujimoto J, Friedman SL, Ikeda K. Adenovirus-mediated expression of BMP-7 suppresses the development of liver fibrosis in rats. Gut 2007; 56: 706-714.
69) Wang LP, Dong JZ, Xiong LJ, Shi KQ, Zou ZL, Zhang SN, Cao ST, Lin Z, Chen YP. BMP-7 attenuates liver fibrosis via regulation of epidermal growth factor receptor. Int J Clin Exp Pathol 2014; 7: 3537-3547.
70) Bi J, Ge S. Potential roles of BMP9 in liver fibrosis. Int J Mol Sci 2014; 15: 20656-20667.
71) Breitkopf-Heinlein K, Meyer C, König C, Gaitantzi H, Addante A, Thomas M, Wiercinska E, Cai C, Li Q, Wan F, Hellerbrand C, Valous NA, Hahnel M, Ehlting C, Bode JG, Müller-Bohl S, Klingmüller U, Altenöder J, Ilkavets I, Goumans MJ, Hawinkels LJ, Lee SJ, Wieland M, Mogler C, Ebert MP, Herrera B, Augustin H, Sánchez A, Dooley S, Ten Dijke P. BMP-9 interferes with liver regeneration and promotes liver fibrosis. Gut 2017; 66: 939-954.